# The importance of groundwater to the upper Columbia River floodplain wetlands

Casey R. Remmer, Rebecca Rooney, Suzanne Bayley & Catriona Leven

View supplementary material ⬈

Published online: 27 Jul 2023.

Submit your article to this journal ⬈

Article views: 24

View related articles ⬈

View Crossmark data ⬈

Taylor & Francis
Taylor & Francis Group

Check for updates

# The importance of groundwater to the upper Columbia River floodplain wetlands

Casey R. Remmer[a] 📙, Rebecca Rooney[a] 📙, Suzanne Bayley[b] 📙 and Catriona Leven[a]

[a]Department of Biology, University of Waterloo, Waterloo, Ontario, Canada; [b]Department of Biological Sciences, University of Alberta, Edmonton, AB, Canada

**ABSTRACT**

The Columbia Wetland complex is a rare example of a North American river system with relatively little disturbance from human infrastructure and is the only undammed portion of the main 2000 km stretch of the Columbia River. Declining river flows in western North America, including the upper Columbia River, have reduced the area of open water wetlands in the floodplain and raised concern that the Columbia Wetlands will not remain viable under increasing climate change. In this study we use water isotopes ($\delta^{18}$O and $\delta^2$H) and electrical conductivity to quantify the proportion of groundwater, river water and precipitation contributing to wetland water balance, as well as the role of evaporation, in the Columbia Wetlands through the spring, summer and fall of 2019. We found strong seasonality of water input sources. Groundwater and precipitation were important in spring and fall, while river water was dominant during the summer. An individual wetlands' location in the floodplain as well as relative connectivity to the river channels influenced its seasonal pattern of input sources. Quantifying the relative contributions of the main input water sources to wetlands provides important new understanding of hydrologic connectivity in the Columbia Wetlands.

**RÉSUMÉ**

Le complexe Columbia Wetland est un exemple rare d'un système fluvial nord-américain avec relativement peu de perturbations par l'infrastructure humaine et est la seule partie sans barrage du tronçon principal de 2000 km du fleuve Columbia. La baisse des débits fluviaux dans l'ouest de l'Amérique du Nord, y compris le cours supérieur du fleuve Columbia, a réduit la superficie des zones humides d'eau libre dans la plaine inondable et fait craindre que les terres humides du Columbia ne restent pas viables dans un contexte de changement climatique croissant. Dans cette étude, nous utilisons les isotopes de l'eau ($\delta^{18}$O et $\delta^2$H) et la conductivité électrique pour quantifier la proportion d'eau souterraine, d'eau de rivière et de précipitations contribuant à l'équilibre hydrique des zones humides, ainsi que le rôle de l'évaporation, dans les zones humides Columbia au printemps, en été et automne 2019. Nous avons constaté une forte saisonnalité des sources d'apport d'eau. L'eau souterraine et les précipitations étaient importantes au printemps et à l'automne, tandis que l'eau des rivières prédominait durant l'été. L'emplacement d'une zone humide individuelle dans la plaine inondable ainsi que la connectivité relative aux canaux de la rivière ont influencé son modèle saisonnier de sources d'apport. La quantification des contributions relatives des principales sources d'eau d'entrée aux zones humides fournit une nouvelle compréhension importante de la connectivité hydrologique dans les zones humides du Columbia

## Introduction

The dominant sources of water in mountain environments are from high precipitation, snowmelt and glaciers (Messerli, Viviroli, and Weingartner 2004; Cooper, Chimner, and Merritt 2012). Most research on mountain hydrology has been on snowpack and glaciers while groundwater was considered a less important source of water. The importance of groundwater as a source of water in mountain environments, contributing to stream flow and alluvial and lowland aquifers is increasingly being acknowledged (Somers and McKenzie 2020). Subsurface flow of groundwater from mountain environments to lowland aquifers is known to be very important, but difficult to quantify (Markovich et al. 2019). Groundwater discharge is highly variable spatially and seasonally and vulnerable to climate change but critically important to montane rivers and wetlands (Huntington and Niswonger 2012; Cooper, Chimner, and Merritt 2012).

The Columbia Wetland complex is a rare example of a North American river system with relatively little disturbance from human infrastructure. It is the only undammed portion of the main 2000 km stretch of the Columbia River and comprises a 26,000 ha Ramsar Wetland of International Importance. The natural flood pulse arrives in June and structures the ecology of the floodplain wetlands. The wetlands are dominated by the seasonal flood pulse (Carli and Bayley 2015, MacDonald 2020), but the relative importance of river water, groundwater discharge and direct precipitation to the water budgets of the Columbia Wetlands is unknown. Generally, groundwater emerges from aquifers and springs at the base of the mountain ranges. In the Columbia Valley, groundwater discharge is derived primarily from unconfined sand and gravel aquifers (UCBGMP, 2021)

Climate change is expected to increase temperatures and evaporation in the region and change precipitation and snowmelt patterns (Utzig 2021). Changes in snowmelt have reduced the flows in western North America (Mote et al. 2005; Schnorbus, Werner, and Bennett 2014; Mote et al. 2018) and in the upper Columbia River in Canada in recent years (Rood et al. 2016; Brahney et al. 2017). Using remote sensing to construct a time series, Hopkinson et al. (2020) found that climate change also reduced the area of open water in wetlands of the Columbia Wetlands complex. There is great concern for the future viability of the Columbia Wetlands given the projected increases in temperature and decreases in river flows.

The stable isotopes of oxygen and hydrogen have long been used to characterize water sources and the influence of evapotranspiration in lakes and wetlands (i.e. Blasch and Bryson 2007; Yi et al. 2008; Wassenaar, Athanasopoulos, and Hendry 2011). The stable isotopes approach has proven particularly valuable in understanding the dynamic hydrology of northern floodplains and remote, wetland-dominated landscapes (e.g. Gibson and Edwards 2002; Brock, Wolfe, and Edwards 2007; MacDonald et al. 2017). For example, water stable isotopes were valuable in quantifying the role of input water sources to water bodies in the Peace-Athabasca Delta (Wolfe et al. 2008, Remmer et al. 2020a,2020b), the Slave River Delta (Brock, Wolfe, and Edwards 2008), and the Old Crow Flats (Turner et al. 2014). Additional insights into hydrological processes in dynamic, wetland-rich landscapes are becoming available as researchers combine stable tracers, such as water isotopes, with statistical analyses underlying source-portioning mixing models commonly used for animal diet differentiation (e.g. Wynants et al. 2020; Kay et al. 2021).

Our overall goal was to use stable isotope tracers to quantify the amount of groundwater, river water, and precipitation inputs to the water budgets of the Columbia Wetlands in the spring, summer and fall. The relative contribution of these water sources likely varies seasonally. We hypothesize that i) snowmelt runoff plays an important role in the spring, ii) that river water inputs coincide with the peak flood pulse in late June and early July, iii) and that groundwater sources are more important in the fall and spring when the river is less influential. We also sought to understand the role of evaporation in determining wetland water levels, and hypothesised that iv) evaporation to inflow ratios would display both spatial (increasing with increased isolation from the river) and seasonal (highest in summer and fall) patterns.

## Methods

### Study area and geographic setting

The upper Columbia River in Canada flows northwest from Columbia Lake between the Rocky Mountains in the east and the Purcell Mountains in the west of southern BC (Figure 1). The entire floodplain is laterally restricted ($\sim$1.5 km wide) but longitudinally continuous from the towns of Invermere, B.C. to Donald, B.C. with a gentle slope, averaging 11.5 cm/km (Makaske et al. 2009). The average spring snow/water equivalent is 500–750 mm in the Purcell Mountains (Hare and Thomas 1974). Above the Nicholson, B.C. gauging station, the drainage of the river is 6660 km$^2$, with a mean annual discharge of 115.1 m$^3$/s and a mean peak discharge (1903–2020) of 435.4 m$^3$/s. Discharge in the upper Columbia River increases in June and early July in response to rainfall and snowmelt, while glacial meltwater constitutes only a minor component of the total discharge (Makaske et al. 2009).

The floodplain is a complex of wetland types dependant on proximity to flood waters from the Columbia River. Some wetlands retain surface water over the winter, while others drain almost completely dry; the different types of wetlands are characterized by different vegetative communities (Rooney, Carli, and Bayley 2013, Carli and Bayley 2015). In the $\sim$50% of years when floodwaters overtop the natural levees, all the wetlands receive the turbid peak floodwaters for a short period of time. During low to moderate flood years, river water will not rise high enough to overtop the levees and will aggrade the flood-basin floor (Filgueira-Rivera, Smith, and Slingerland 2007). During years with low to moderate peak flows (or later in the season), wetlands are more isolated from the main flood peak by natural levees and beaver dams, such
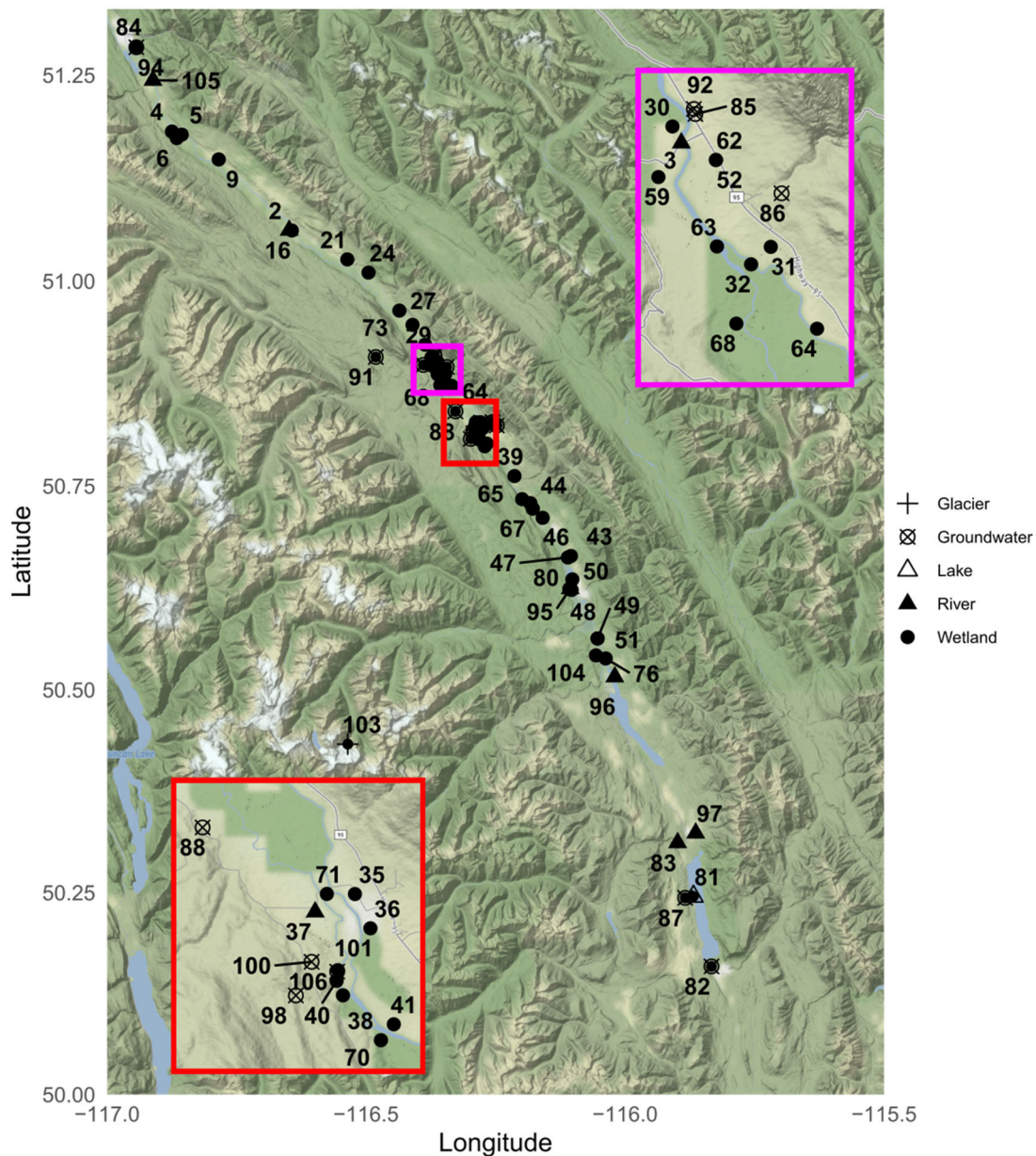
**Figure 1.** Location of sampling sites in the upper Columbia Valley, British Columbia. Rivers are denoted as a triangle, wetlands as a circle, groundwater as a cross and Columbia Lake as a square. Note that this section of the Columbia river flows from South-east to northwest. The regions within the red and purple boxes are expanded in the insets so that overlapping points can be visualized. This map was created using R version 4.2.2. Map tiles by Stamen Design, under CC BY 3.0. Data by OpenStreetMap, under ODbL.

that they only receive water through gaps in the levees or from groundwater. Thus, some wetlands are more isolated and consequently receive less flood water, have lower water levels and different vegetation characteristics than wetlands well-connected to the main river. All the wetlands show some indication of groundwater in all seasons but the importance of the groundwater to the water budget is unknown and likely differs among types of wetland basins.

The Columbia River Valley ranges from 4.8 to 9.6 km wide with a physiology typical of glaciated valleys. It is flanked by the Purcell mountain ranges to

the west and the Kootenay, Brisco and Stanford Ranges to the east. These mountain ranges primarily consist of limestone and shale, while the river valley is underlain by glacial till and silt deposits (Columbia Wetland Stewardship Partners 2009; Figure S1).

### Sample collection

Water samples were collected in collaboration with the Columbia Wetlands Stewardship Partners during the spring (50 samples, April 26th to May 19th), summer during peak flood (59 samples, June 4th to June 26th)

and fall (57 samples, Sept 14th to Oct. 20th) of 2019. In the spring, 27 wetland samples were collected along with 8 samples from the river and its channels and 14 springs/wells; in summer, 41 wetland water samples were collected along with 8 samples from the river and its channels and 11 springs/wells, in fall, 39 wetland water samples were collected along with 5 samples from the river and its channels and 13 springs/wells. Water samples were collected from each site at a depth of ∼10 cm and stored in sealed 30 ml high-density polyethylene bottles. Samples were collected by community volunteers under the supervision and guidance of Dr. Bayley. Wetlands and rivers were sampled by wading to an accessible depth from the shoreline, and wetlands are assumed to be well mixed. The precise depths of sampled wells are not known but is estimated to be ∼30 m, except for site 93 which is ∼6 m. Numbering reflects multiple years of data collection during which not all sites were accessed. To keep internal documentation consistent, the sites are labeled according to the meta-numbering system.

Wetland water isotope compositions were measured by Off-Axis Integrated Cavity Output Spectroscopy (O-AICOS). All samples were analyzed at the University of Waterloo – Environmental Isotope Laboratory (UW-EIL). Isotope compositions are expressed as δ-values, representing deviations in per mil (‰) from Vienna Standard Mean Ocean Water (VSMOW) such that $\delta_{sample} = [(R_{sample}/R_{VSMOW}) - 1] \times 10^3$, where R is the $^{18}O/^{16}O$ or $^2H/^1H$ ratio in the sample and VSMOW. Results of $\delta^{18}O$ and $\delta^2H$ analyses are normalized to $-55.5‰$ and $-428‰$, respectively, for Standard Light Antarctic Precipitation (Coplen 1996). Isotope compositions were measured using 8 injections per sample analysis with the first two being rejected, such that the remaining six are averaged for the final value. The standard ranges are $-21.28$ to $-2.99$ for $^{18}O$, and $-165.7$ to $-9.9$ for $^2H$. Standards are analyzed in four groups across the run with one at the beginning, a second approximately 1/3 (37% mark of run), third group approximately 2/3 (67% mark of run) and final group at the end. Check standards are included in the analysis starting at the top of the run, placed every 8th in a full run size of 36 discrete samples and ending with check standard (Position:1,9,17,25,33,37) Across two runs the standard deviation of the check standards were $+/-$ 0.1 and 0.11 $^{18}O$, and $+/-0.61$ and 0.31 for $^2H$. Normalization was done with Los Gatos Research Liquid Water Isotope Analyzer Post Analysis software (LGR LWIA Post Analysis) version 4.5.0.6. Settings within the software are to use a Cubic Spline Fitting for standard normalization. Uncertainty was calculated by using the normalized data (standards

calibrated against international VSMOW Standards) and taking the difference of normalized data against known standard value. The standard deviation is determined between all the differences of respective standard values and averaged as a final uncertainty. Analytical uncertainties are ±0.09‰ for $\delta^{18}O$ and ±0.4‰ for $\delta^2H$. Measurements of electrical conductivity were obtained using a Thermo Fisher Scientific Orion[TM] Versa Star Pro[TM] pH/ISE/Conductivity/Dissolved Oxygen Multiparameter Benchtop Meter with the Orion[TM] DuraProbe[TM] 4-Cell Conductivity Probe (model 013005MD) and are reported in μS/cm. Orion Application Solution Orion 011007 1413 μS/cm calibration solution was used to calibrate at the beginning of each of 4 days of measurement.

## Meteorological calculations

Relative humidity ($h$) and temperature ($T$) were calculated as the average (monthly) evaporation-flux-weighted values during 2019, using climate data from Environment and Climate Canada (station number 71305; www.climate.weather.gc.ca) and the National Research Council of Canada (http://www.nrc-cnrc.gc.ca/eng/services/sunrise/). The average ice-free season $h$ and $T$ were flux-weighted based on potential evapotranspiration determined by Thornthwaite (1948):

$$h_{flux} = \sum \frac{(h \times E_t)}{(E_t)} \tag{1}$$

$$T_{flux} = \sum \frac{(T_a \times E_t)}{(E_t)} \tag{2}$$

where $T_a$ is the monthly average temperature and $E_t$ is the monthly total evaporation. $E_t$ was calculated using the equation:

$$E_t = 1.6 \cdot \frac{L}{12} \cdot \frac{N}{30} \left[ \frac{10 \cdot T_a}{I} \right]^a \tag{3}$$

where $L$ is the average day length in hours in a month, $N$ is the number of days in the month, $I$ is the annual heat index and $a$ is a calculated coefficient. $I$ was calculated as the total of each ice-free month using the equation:

$$I = \sum I_i \tag{4}$$

and $I_i$ was calculated using the equation:

$$I_i = \left( \frac{T_\alpha}{5} \right)^{1.5} \tag{5}$$

and $a$ was calculated using the equation:

$$a = 0.49 + 0.0179 \cdot I - 7.71 \cdot 10^{-5} \cdot I^2 + 6.75 \cdot 10^{-7} \cdot I^3 \tag{6}$$

## Isotopic framework

An isotopic framework was developed to interpret the dominant hydrological processes influencing wetlands. Isotope framework parameters were calculated (in decimal notation) using approaches described in Gonfiantini (1986), Gibson and Edwards (2002), Edwards et al. (2004), and Yi et al. (2008), which are based on the linear resistance model of Craig and Gordon (1965). The framework consists of two linear trends. The Global Meteoric Water Line (GMWL), described by $\delta^2H = 8\ \delta^{18}O + 10$, represents the observed global relationship between $\delta^{18}O$ and $\delta^2H$ in amount-weighted annual precipitation. In a region, the isotopic composition of precipitation will cluster along a Local Meteoric Water Line (LMWL). For the Columbia Valley the LMWL was approximated by $\delta^2H = 8.21\ \delta^{18}O - 9.36$, based on precipitation collected at the nearest Global Network of Isotopes in Precipitation (GNIP) site (Calgary, Alberta). The Local Evaporation Line (LEL) represents the trajectory of surface water undergoing evaporation (Gibson and Edwards 2002). Here we use a predicted LEL, based on the linear resistance model of Craig and Gordon (1965), which allows water isotope compositions to be interpreted independently based on their position along or about the LEL. This is advantageous to the more common technique of applying linear regression through measured water isotope compositions, as it allows isotope compositions to be interpreted independently based on their position along (degree of evaporation) and about (i.e. above/below; relative influence of different input waters such as snowmelt and rainfall) the LEL.

For the Columbia Valley, the predicted LEL was determined as the line intersecting the isotope composition of precipitation ($\delta_P$), the isotope composition of a terminal basin at steady-state ($\delta_{SSL}$) and the theoretical limiting non-steady-state composition of a water body approaching complete desiccation ($\delta^*$). $\delta_P$ was obtained from the Online Isotopes in Precipitation Calculator (Bowen 2016; Bowen and Revenaugh 2003; IAEA/WMO 2015. $\delta^*$ was calculated from Gonfiantini (1986):

$$\delta^* = \frac{h \cdot \delta_{AS} + \varepsilon_k + \frac{\varepsilon^*}{\alpha^*}}{h - \varepsilon_k - \frac{\varepsilon^*}{\alpha^*}} \qquad (7)$$

where $h$ is the relative humidity (see EQ. S1), $\delta_{AS}$ is the isotope composition of atmospheric moisture for the ice-free season (Gibson et al), $\delta_k$ is the kinetic separation factor between liquid and vapour phases, $\delta^*$ is the equilibrium separation factor between liquid and vapour phases, and $\alpha^*$ is the equilibrium liquid-vapour isotope fractionation factors (Horita and Wesolowski 1994). $\alpha^*$ for $\delta^2H$ and $\delta^{18}O$ was derived from the equations described by Horita and Wesolowski (1994):

$$1000\ ln\ ln\ ln\ \alpha^* = 1158.8\left(\frac{T^3}{10^9}\right) - 1620.1\left(\frac{T^2}{10^6}\right)$$
$$+ 794.84\left(\frac{T^3}{10^3}\right) + 2.9992\left(\frac{10^9}{T^3}\right)$$
$$- 161.04 \qquad (8)$$

for $\delta^2H$ and

$$1000\ ln\ ln\ ln\ \alpha^* = -7.685 + 6.7123\left(\frac{10^3}{T}\right)$$
$$- 1.6664\left(\frac{10^6}{T^2}\right)$$
$$+ 0.35041\left(\frac{10^9}{T^3}\right) \qquad (9)$$

for $\delta^{18}O$ where $T$ represents the interface temperature in degrees Kelvin. The equilibrium separation factor between liquid and vapour phases is expressed as

$$\varepsilon^* = \alpha^* - 1 \qquad (10)$$

and the kinetic separation factor between liquid and vapour phases is expressed as

$$\varepsilon_k = 0.0125(1 - h) \qquad (11)$$

for $\delta^2H$ and

$$\varepsilon_k = 0.0142(1 - h) \qquad (12)$$

for $\delta^{18}O$, where h is the relative humidity (Gonfiantini 1986). Isotope composition of atmospheric moisture for the ice-free season ($\delta_{AS}$) was calculated using the equation from Gibson and Edwards (2002) and is assumed to be in equilibrium with evaporation-flux-weighted summer precipitation

$$\delta_{AS} = \frac{\delta_{PS} - \varepsilon^*}{\alpha^*} \qquad (13)$$

The calculated limiting steady-state isotopic composition ($\delta_{SSL}$) was obtained from the Craig-Gordon equation for the isotopic composition ($\delta_E$) of the evaporating flux from a lake ($\delta_L$) undergoing steady-state evaporation (also for $\delta$, $\epsilon$ and h values in decimal notation)

$$\delta_E = \frac{\frac{(\delta_L - \varepsilon^*)}{\alpha^*} - h \cdot \delta_{AS} - \varepsilon_k}{1 - h + \varepsilon_k} \qquad (14)$$

for the special case in which $\delta_E = \delta_P$.

Results of the isotope framework calculations are reported in Table 1.

**Table 1.** Values used for calculations of the isotope framework, with references and equation numbers where appropriate.

| Parameter | Value | Source | Equation |
|---|---|---|---|
| h (%) | 69.52 | Environment Canada | EQ.1 |
| T (°C) | 14.42 | | EQ.2 |
| $\alpha^*$ ($^{18}O$, $^2H$) (‰) | 1.0103, 1.0912 | | EQ.8, EA.9 |
| $\varepsilon^*$ ($^{18}O$, $^2H$) (‰) | 10.32, 91.15 | | EQ.10 |
| $\varepsilon_k$ ($^{18}O$, $^2H$) (‰) | 4.33, 3.81 | | EQ.11, EQ.12 |
| $\delta_{As}$ ($^{18}O$, $^2H$) (‰) | −21.46, −164.92 | | EQ.13 |
| $\delta_P$ ($^{18}O$, $^2H$) (‰) | −14.12, −111.15 | OIPC | |
| $\delta^*$ ($^{18}O$, $^2H$) (‰) | −0.55, −44.92 | | EQ.7 |
| $\delta_{SSL}$ ($^{18}O$, $^2H$) (‰) | −4.79, −67.22 | | EQ. 14 |
| LEL Slope | 4.7 | | |
| LEL Intercept | −44.68 | | |

## Water balance metrics

For each wetland, the isotopic composition of lake input water ($\delta_I$) was estimated as the intersection of a lake specific evaporation line through $\delta_E$ and $\delta^*$ and the GMWL, utilizing the coupled isotope tracer approach (Yi et al. 2008). Evaporation-to-inflow ratios (E/I), described by Yi et al. (2008) and others, where calculated as

$$\frac{E}{I} = \frac{(\delta_I - \delta_L)}{(\delta_E - \delta_L)} \qquad (15)$$

and provide an index of water balance.

## Statistical analysis

Mixing equations for stable isotopic data within a Bayesian framework were originally developed to differentiate food sources in animal diets but are now being broadly used across ecology and biology to estimate the proportion of sources contributing to a mixture (Parnell et al. 2010). The simmr package in R uses a Bayesian framework to estimate the proportion of a mixture that can be attributed to a suite of potential sources, based on selected tracers. Here we use measurements of $\delta^2H$, $\delta^{18}O$ and electrical conductivity to calculate the estimated proportion of wetland input water that can be attributed to either groundwater sources, river flooding or precipitation. Details of the stable isotope mixing model can be found in Parnell et al. (2010, 2013). For this study, the calculated $\delta^2H$ and $\delta^{18}O$ and measured electrical conductivity of each wetland were input into the model as the mixtures. Electrical conductivity was included to assist in differentiating isotopically depleted river water from isotopically depleted groundwater, as groundwater is known to have higher electrical conductivity due to interactions with the limestone bedrock of the area (see S.2). To calculate the mean and standard deviation of the river, groundwater and rain input sources, all available measurements of isotopic composition and electrical

conductivity were used. For the river $n = 8$ in spring, $n = 8$ in summer, $n = 6$ in fall and for groundwater $n = 14$ in spring, $n = 9$ in summer, $n = 9$ in fall. For rainfall, direct measurements were not possible. Isotopic composition of rainfall was estimated using mean and standard deviation of the modelled monthly value of each wetland site extracted from the OIPC v3.2 data base (Bowen and Revenaugh 2003, Bowen et al. 2005) for each of the three sampling periods (April -May = spring, June-July = summer, August-September = fall). Modelled values of the isotopic composition of rainfall are well established (Bowen and Revenaugh 2003). To generate an estimate of the specific electrical conductivity of rainfall, data from the two closest National Ecological Observatory Network sites (Wyoming, northern Rockies [D12-WY] and Washington [D16-WA]) collected during the sampling months in 2019 were used (NEON, 2021). Given that rain has very low and temporally stable electrical conductivity, relative to river and groundwater (Zuecco et al. 2018) this estimate was considered sufficient for the analysis. The model was run separately for each sampling period (spring, summer and fall) and proportions were calculated for each wetland individually. In cases where wetlands did not fall within the bounds of the source tracers, these sites were removed from the analysis (Tables 2 and 3).

## Results

### Water isotopes

During the spring, river water and groundwater isotopic compositions plot below the predicted LEL (Figure 2). The groundwater measurements primarily cluster on the LMWL below $\delta_P$, suggesting the groundwater is composed of isotopically depleted snowmelt ($\delta^2H = -146.8$ and $\delta^{18}O = -19.38$; OIPC). River water measurements similarly plot below the LEL, and lie along the LMWL, a possible indicator of input of isotopically depleted precipitation. The exception to this is river site 83 (i.e. Dutch Creek), which was experiencing evaporation. All the wetlands plot below the LEL, indicating the dominance of snowmelt and snowmelt derived water sources. Spread of wetlands along the LEL suggests varying influence of evaporation during the spring period. Some wetlands sites did not contain enough water to be sampled during the spring due to over-winter drawdown in these floodplain marshes. Columbia Lake, situated at the headwaters of the Columbia River, plots within the groundwater cluster on the

**Table 2.** Site type, location, collection date, water isotope composition and electrical conductivity of sites in the upper Columbia Valley sampled in spring, summer and fall of 2019.

| Site number | Site type | Easting | Northing | Spring Date collected | δ18O | δ2H | Electrical conductivity | Summer Date collected | δ18O | δ2H | Electrical conductivity | Fall Date collected | δ18O | δ2H | Electrical conductivity |
|---|---|---|---|---|---|---|---|---|---|---|---|---|---|---|---|
| 2 | River | 524643 | 5656772 | 07-May | −19.56 | −149.63 | 288 | 14-Jun | −19.95 | −152.00 | 184 | 14-Sep | −18.72 | −143.22 | 203 |
| 3 | River | 544200 | 5639356 | 05-May | −19.16 | −147.38 | 351 | 06-Jun | −19.93 | −152.36 | 204 | 15-Sep | −18.58 | −141.38 | 241 |
| 4 | Wetland | 508765 | 5670042 | 12-May | −18.48 | −143.62 | 229 | 15-Jun | −17.48 | −139.60 | 241 | 04-Oct | −17.47 | −138.58 | 277 |
| 5 | Wetland | 510074 | 5669625 | – | – | – | – | 15-Jun | −19.40 | −149.65 | 191 | 04-Oct | −13.73 | −116.86 | – |
| 6 | Wetland | 509418 | 5669160 | 12-May | −13.21 | −120.67 | 183 | 15-Jun | −18.80 | −146.73 | 221 | 04-Oct | −13.73 | −116.86 | 182 |
| 9 | Wetland | 515082 | 5666300 | 02-May | −19.24 | −147.40 | 320 | 14-Jun | −18.03 | −144.08 | 250 | 18-Sep | −14.55 | −120.80 | 269 |
| 16 | Wetland | 525002 | 5656741 | 02-May | −15.99 | −135.29 | 257 | 14-Jun | −19.87 | −151.52 | 197 | 14-Sep | −15.26 | −124.03 | 238 |
| 21 | Wetland | 532535 | 5652873 | 05-May | −16.81 | −136.03 | 356 | 06-Jun | −16.89 | −136.35 | 272 | 14-Sep | −16.36 | −131.38 | 319 |
| 24 | Wetland | 535422 | 5651111 | 02-May | −17.68 | −140.38 | 728 | 06-Jun | −19.96 | −152.64 | 205 | 18-Sep | −18.02 | −138.08 | 296 |
| 27 | Wetland | 541432 | 5644074 | – | – | – | – | 06-Jun | −19.98 | −152.56 | 204 | 11-Oct | −14.75 | −122.01 | 320 |
| 29 | Wetland | 543167 | 5641399 | – | – | – | – | 06-Jun | −18.58 | −147.00 | 253 | 11-Oct | −10.63 | −103.44 | 343 |
| 30 | Wetland | 544030 | 5639666 | 28-Apr | −7.34 | −90.92 | 244 | 06-Jun | −20.04 | −152.21 | 197 | 18-Sep | −15.98 | −128.03 | 190 |
| 31 | Wetland | 545913 | 5637403 | 26-Apr | −14.30 | −126.13 | 416 | 08-Jun | −17.68 | −141.24 | 296 | 18-Sep | −17.48 | −137.62 | 549 |
| 32 | Wetland | 545543 | 5637069 | 11-May | −16.81 | −137.49 | 353 | – | – | – | – | 01-Oct | −18.30 | −140.85 | 282 |
| 35 | Wetland | 550776 | 5630949 | 26-Apr | −15.77 | −132.25 | 1187 | 04-Jun | −14.20 | −126.46 | 1216 | 15-Sep | −11.09 | −110.86 | 1276 |
| 36 | Wetland | 551130 | 5630189 | 26-Apr | −18.35 | −144.42 | – | 04-Jun | −20.34 | −154.56 | 203 | 18-Sep | −16.67 | −132.33 | 466 |
| 37 | River | 549892 | 5630542 | 05-May | −14.52 | −126.60 | 337 | 04-Jun | −20.44 | −155.23 | 190 | 15-Sep | −19.01 | −143.78 | 257 |
| 38 | Wetland | 550531 | 5628689 | 03-May | −15.19 | −131.01 | 323 | 04-Jun | −12.14 | −117.12 | 314 | 15-Sep | −13.10 | −116.81 | 244 |
| 39 | Wetland | 555476 | 5623684 | 28-Apr | −13.81 | −122.25 | 397 | 05-Jun | −17.77 | −143.14 | 315 | 17-Sep | −11.37 | −107.70 | 543 |
| 40 | Wetland | 550385 | 5629010 | – | – | – | – | 04-Jun | −19.95 | −152.29 | 319 | 06-Oct | −18.51 | −145.92 | 706 |
| 41 | Wetland | 551673 | 5628055 | – | – | – | – | 14-Jun | −17.87 | −142.08 | 408 | – | – | – | – |
| 43 | Wetland | 563287 | 5612893 | 27-Apr | −11.67 | −113.89 | 350 | 15-Jun | −18.61 | −144.21 | 355 | 05-Oct | −13.71 | −122.07 | 372 |
| 44 | Wetland | 557678 | 5620027 | – | – | – | – | 14-Jun | −19.57 | −148.71 | 293 | 03-Oct | −18.48 | −144.70 | 314 |
| 46 | Wetland | 559375 | 5618042 | – | – | – | – | 14-Jun | −18.48 | −146.15 | 244 | 24-Sep | −14.01 | −124.03 | 250 |
| 47 | Wetland | 562874 | 5612685 | 01-May | −11.52 | −112.20 | 446 | 09-Jun | −19.09 | −149.09 | 256 | 05-Oct | −7.56 | −94.96 | 425 |
| 48 | Wetland | 563443 | 5608264 | 01-May | −15.33 | −129.73 | 370 | 09-Jun | −8.16 | −99.12 | 285 | 05-Oct | −6.30 | −84.65 | 375 |
| 49 | Wetland | 567072 | 5601686 | 06-May | −14.09 | −126.22 | 505 | 15-Jun | −13.70 | −124.54 | 435 | 20-Sep | −13.11 | −119.10 | 543 |
| 50 | Wetland | 563526 | 5609698 | – | – | – | – | 09-Jun | −19.44 | −149.22 | 284 | 04-Oct | −16.47 | −127.84 | 288 |
| 51 | Wetland | 567072 | 5601686 | 08-May | −15.53 | −131.56 | 509 | 05-Jun | −20.05 | −151.57 | 189 | 04-Oct | −16.71 | −133.34 | 364 |
| 52 | Wetland | 544859 | 5639039 | 19-May | −13.55 | −122.28 | 468 | – | – | – | – | – | – | – | – |
| 59 | Wetland | 543772 | 5638706 | – | – | – | – | 06-Jun | −19.99 | −152.53 | 182 | 18-Sep | −15.45 | −124.88 | 290 |
| 62 | Wetland | 544859 | 5639039 | 03-May | −12.95 | −120.45 | 342 | 08-Jun | −12.42 | −119.80 | 284 | 18-Sep | −8.45 | −98.84 | 317 |
| 63 | Wetland | 544893 | 5637402 | 11-May | −20.42 | −154.19 | 199 | 09-Jun | −12.26 | −118.24 | 173 | 01-Oct | −11.22 | −111.59 | 211 |
| 64 | Wetland | 546804 | 5635861 | – | – | – | – | 09-Jun | −19.10 | −148.50 | 265 | 01-Oct | −12.55 | −114.85 | 283 |
| 65 | Wetland | 556550 | 5620549 | – | – | – | – | 14-Jun | −19.95 | −152.51 | 209 | 24-Sep | −17.43 | −134.72 | 192 |
| 67 | Wetland | 558030 | 5619271 | – | – | – | – | 14-Jun | −20.42 | −153.73 | 196 | 24-Sep | −18.61 | −141.70 | 245 |
| 68 | Wetland | 545273 | 5635944 | – | – | – | – | 09-Jun | −19.88 | −151.59 | 237 | 01-Oct | −19.09 | −146.62 | 253 |
| 70 | Wetland | 551389 | 5627697 | 28-April | −11.33 | −112.42 | 191 | 14-Jun | −19.42 | −150.28 | 232 | 24-Sep | −13.52 | −117.21 | 273 |
| 71 | Wetland | 550149 | 5630945 | 03-May | −17.45 | −137.61 | 303 | 04-Jun | −19.28 | −149.32 | 200 | 15-Sep | −13.87 | −120.35 | 269 |
| 73 | Wetland | 539633 | 5645997 | – | – | – | – | 06-Jun | −20.20 | −153.88 | 196 | 11-Oct | −15.29 | −121.78 | 250 |
| 76 | Wetland | 568220 | 5598967 | 01-May | −14.68 | −127.42 | 397 | 14-Jun | −17.63 | −139.16 | 423 | 20-Oct | −17.06 | −134.19 | 425 |
| 80 | Wetland | 563138 | 5608395 | 27-Apr | −15.43 | −125.97 | 297 | 15-Jun | −20.69 | −156.54 | 149 | – | – | – | – |
| 81 | Lake | 580717 | 5566532 | 07-May | −19.35 | −146.28 | 341 | 04-Jun | −16.09 | −131.20 | 307 | 28-Sep | −14.94 | −123.93 | 369 |
| 82 | Spring | 583348 | 5556946 | 08-May | −19.84 | −151.20 | 357 | 04-Jun | −19.55 | −146.86 | 371 | 28-Sep | −19.30 | −146.45 | 389 |
| 83 | River | 578436 | 5573872 | 07-May | −10.48 | −108.56 | 226 | 12-Jun | −20.6 | −153.26 | 157 | 28-Sep | −19.29 | −147.13 | 208 |
| 84 | Wetland | 503947 | 5681387 | 12-May | −19.61 | −151.93 | 1193 | 15-Jun | −8.53 | −99.40 | 1433 | 10-Oct | −8.29 | −93.08 | 1366 |
| 85 | Well | 544461 | 5639905 | 03-May | −18.92 | −144.84 | 640 | 12-Jun | −19.68 | −152.71 | 674 | 09-Oct | −20.02 | −152.01 | 673 |
| 86 | Spring | 546108 | 5638419 | 03-May | −19.49 | −148.85 | 450 | 26-Jun | −18.91 | −145.39 | 451 | 03-Oct | −18.81 | −143.94 | 491 |

(continued)

**Table 2.** Continued.

| Site number | Site type | Easting | Northing | Spring Date collected | δ¹⁸O | δ²H | Electrical conductivity | Summer Date collected | δ¹⁸O | δ²H | Electrical conductivity | Fall Date collected | δ¹⁸O | δ²H | Electrical conductivity |
|---|---|---|---|---|---|---|---|---|---|---|---|---|---|---|---|
| 87 | Spring | 579586 | 5566317 | 14-May | −19.65 | −149.67 | 379 | 04-Jun | −19.21 | −149.2 | 398 | 27-Sep | −19.64 | −149.24 | 442 |
| 88 | Spring Pond | 547407 | 5632366 | 04-May | −19.18 | −146.62 | 374 | – | – | – | – | – | – | – | – |
| 89 | Spring Pond | 552401 | 5631018 | 17-May | −19.04 | −146.60 | 686 | – | – | – | – | – | – | – | – |
| 90 | Spring Pond | 552409 | 5630895 | 17-May | −17.92 | −143.87 | 694 | – | – | – | – | – | – | – | – |
| 91 | Spring Pond | 535673 | 5650949 | 05-May | −19.27 | −150.17 | 644 | – | – | – | – | – | – | – | – |
| 92 | Spring | 544433 | 5640001 | 07-May | −19.04 | −147.73 | 731 | 12-Jun | −19.42 | −150.38 | 754 | 08-Oct | −19.40 | −149.43 | 861 |
| 93 | Well | 542937 | 5638661 | 05-May | −16.05 | −135.73 | 366 | 12-Jun | −19.33 | −148.81 | 429 | 20-Oct | −19.08 | −144.91 | 524 |
| 94 | Well | 503947 | 5681387 | 04-May | −19.07 | −146.05 | 510 | 12-Jun | −15.91 | −133.78 | 548 | 18-Sep | −17.34 | −140.51 | 680 |
| 95 | River | 563248 | 5608425 | 06-May | −17.92 | −140.59 | 356 | 15-Jun | −20.32 | −152.53 | 207 | – | – | – | – |
| 96 | River | 569494 | 5596464 | 06-May | −19.16 | −147.40 | 406 | 14-Jun | −18.32 | −142.78 | 310 | – | – | – | – |
| 97 | River | 580896 | 575229 | 07-May | −18.82 | −145.46 | 263 | 12-Jun | −19.78 | −150.45 | 189 | 28-Sep | −18.76 | −142.39 | 240 |
| 98 | Spring | 549479 | 5628676 | 11-May | −19.35 | −147.40 | 543 | 23-Jun | −19.01 | −147.56 | 605 | 17-Sep | −18.98 | −145.79 | 659 |
| 99 | Spring | 553001 | 5630529 | 17-May | −20.72 | −161.57 | 653 | 16-Jun | −19.28 | −148.42 | 735 | 05-Oct | −19.42 | −147.94 | 805 |
| 100 | Well | 549823 | 5629429 | 11-May | −22.42 | −171.23 | 876 | 13-Jun | −20.95 | −163.22 | 882 | 20-Oct | −20.78 | −161.77 | 836 |
| 101 | Wetland | 550412 | 5629249 | 03-Mar | −16.37 | −136.27 | 778 | 04-Jun | −13.17 | −124.98 | 1131 | 06-Oct | −10.34 | −107.81 | 1027 |
| 103 | Glacier | 533003 | 5586912 | – | – | – | – | 19-Jul | −20.61 | −153.23 | 23 | – | – | – | – |
| 104 | Wetland | 566883 | 5599369 | 07-May | −16.24 | −135.87 | 482 | 11-Jun | −16.50 | −137.00 | 402 | 03-Oct | −16.93 | −138.13 | 585 |
| 105 | River | 506185 | 576951 | – | – | – | – | 15-Jun | −20.07 | −153.44 | 165 | 14-Oct | −19.00 | −146.14 | 271 |

Note: Not all sites could be surveyed in all seasons due to inaccessibility, such missing data is indicated by -.

LMWL, as is expected during the winter and spring, when evaporative enrichment is minimal.

In the summer, river water isotopic compositions displayed less variability and clustered tightly along the LWML, slightly below the groundwater samples on average. This accords with our expectations, as this sampling in summer occurred during peak river flow, when floodwaters would homogenize the river water chemistry. A sample of Columbia Glacier meltwater plots within the cluster of river water samples, indicating that glacial melt, along with similarly depleted high-elevation snowpack melt, may be a driver of river water isotopic depletion during summer. The overlap between river water and groundwater may be indicative of frequent exchange between these two sources during periods of high water and hydrologic connectivity. All the wetlands sampled in the summer plot below the LEL and the majority plot near the groundwater and river water compositions, suggesting a diminished evaporative influence during this period and a predominance of river and groundwater derived water in these basins. This aligns with the summer river flood pulse and indicates high connectivity with the river system during this period. Columbia Lake moved up the LMWL, possibly due to increasing influence of rainfall and evaporation on this larger water body.

In the fall, river and groundwater samples continue to cluster and overlap along the LMWL below $\delta_P$. Wetlands show greater variability along the LEL as evaporative enrichment influences isotopic composition. Wetlands also primarily plot along, rather than below, the LEL, indicating an increase in the influence of rainfall relative to the previous seasons. Columbia Lake plots further along the LEL, indicating increased evaporative influence as the ice-free season progresses into fall.

To further investigate the role of snowmelt in spring groundwater, we generated boxplots of $\delta^{18}O$, $\delta^2H$ and electrical conductivity for each of the input water sources in each sampling period and the modelled winter precipitation (snow) values at each wetland (plotted on the spring graph), using the same method used for rainfall (Figure 3). The electrical conductivity of snow could not be estimated from the available data. Overlap between the $\delta^{18}O$ values of groundwater and snow, both of which occupy a relatively small range of values, suggests that groundwater is derived from snowmelt. This relationship is not as strong for $\delta^2H$, likely due to difference in fractionation effects, however groundwater and snowmelt have the most depleted ranges. To further investigate

**Table 3.** The proportion of each of three potential source waters contributing to wetland sites in the upper Columbia Valley wetlands sampled in 2019.

| Site number | Spring GW % | Spring River % | Spring Rain % | Summer GW % | Summer River % | Summer Rain % | Fall GW % | Fall River % | Fall Rain % |
|---|---|---|---|---|---|---|---|---|---|
| 4 | 34.7 | 34.2 | 31.2 | 30.1 | 42.0 | 27.9 | 32.7 | 45.1 | 22.2 |
| 5 | not sampled | | | 13.2 | 78.8 | 8.1 | missing data | | |
| 6 | 7.6 | 52.6 | 39.8 | 19.0 | 68.7 | 12.3 | 20.1 | 4.1 | 75.8 |
| 9 | 44.6 | 37.2 | 18.2 | 29.6 | 51.5 | 18.9 | 29.9 | 5.4 | 64.7 |
| 16 | 24.9 | 37.7 | 37.4 | 12.1 | 82.2 | 5.7 | 30.3 | 11.4 | 58.2 |
| 21 | 37.5 | 36.2 | 26.2 | 37.8 | 27.6 | 34.6 | 43.7 | 16.2 | 40.1 |
| 24 | 76.7 | 13.0 | 10.4 | 12.2 | 82.7 | 5.0 | 28.3 | 54.5 | 17.3 |
| 27 | not sampled | | | 12.1 | 82.8 | 5.1 | 34.3 | 5.2 | 60.5 |
| 29 | not sampled | | | 25.9 | 61.7 | 12.4 | 77.8 | 0.9 | 21.3 |
| 30 | removed | | | 11.5 | 83.4 | 5.1 | 22.9 | 29.0 | 48.2 |
| 31 | 23.2 | 66.2 | 10.6 | 40.3 | 36.4 | 23.4 | 64.3 | 14.4 | 21.2 |
| 32 | 38.3 | 35.4 | 26.3 | not sampled | | | 21.3 | 67.5 | 11.2 |
| 36 | missing data | | | 10.7 | 85.3 | 3.9 | 53.7 | 11.9 | 34.4 |
| 38 | 22.7 | 55.3 | 22.0 | 31.0 | 3.2 | 65.9 | 23.4 | 2.3 | 74.3 |
| 39 | 17.7 | 72.8 | 9.5 | 44.0 | 36.1 | 19.9 | 94.0 | 1.2 | 4.8 |
| 40 | not sampled | | | 34.9 | 60.0 | 5.1 | 80.6 | 12.0 | 7.5 |
| 43 | 9.1 | 82.2 | 8.7 | 46.7 | 39.1 | 14.2 | 36.2 | 2.6 | 61.2 |
| 44 | not sampled | | | 28.8 | 63.9 | 7.3 | 30.7 | 62.2 | 7.1 |
| 46 | not sampled | | | 25.3 | 60.6 | 14.1 | 31.1 | 4.2 | 64.7 |
| 47 | 12.0 | 82.6 | 5.3 | 23.4 | 67.9 | 8.8 | removed | | |
| 48 | 26.2 | 56.4 | 17.4 | 43.6 | 1.3 | 55.1 | removed | | |
| 49 | 36.0 | 55.1 | 8.9 | 45.5 | 4.2 | 50.3 | 45.7 | 1.7 | 52.6 |
| 50 | not sampled | | | 27.3 | 65.3 | 7.4 | 34.6 | 21.5 | 43.9 |
| 51 | 49.4 | 36.0 | 14.7 | 11.1 | 83.5 | 5.4 | 46.4 | 19.0 | 34.6 |
| 52 | 25.0 | 67.4 | 7.6 | not sampled | | | not sampled | | |
| 59 | not sampled | | | 10.8 | 84.0 | 5.1 | 35.2 | 10.0 | 54.8 |
| 62 | 11.9 | 76.9 | 11.1 | 29.9 | 3.7 | 66.5 | removed | | |
| 63 | 44.9 | 38.8 | 16.4 | 20.1 | 4.6 | 75.3 | 16.8 | 1.0 | 82.1 |
| 64 | not sampled | | | 24.8 | 66.1 | 9.1 | 24.2 | 1.6 | 74.2 |
| 65 | not sampled | | | 12.9 | 82.0 | 5.1 | 11.0 | 62.7 | 26.3 |
| 67 | not sampled | | | 10.6 | 85.3 | 4.1 | 12.0 | 80.6 | 7.4 |
| 68 | not sampled | | | 15.9 | 78.6 | 5.5 | 20.1 | 76.5 | 3.4 |
| 70 | 5.5 | 71.0 | 23.4 | 17.7 | 75.0 | 7.2 | 26.3 | 2.6 | 71.1 |
| 71 | 35.3 | 33.6 | 31.1 | 14.7 | 76.8 | 8.5 | 28.4 | 3.5 | 68.1 |
| 73 | not sampled | | | 10.5 | 85.1 | 4.3 | 29.6 | 10.3 | 60.1 |
| 76 | 24.1 | 63.4 | 12.5 | 56.7 | 20.7 | 22.6 | 51.8 | 17.7 | 30.4 |
| 80 | 18.8 | 56.8 | 24.4 | 9.1 | 87.7 | 3.2 | not sampled | | |
| 101 | 79.2 | 11.6 | 9.1 | removed | | | removed | | |
| 104 | 51.8 | 30.1 | 18.1 | 54.3 | 14.6 | 31.1 | 66.9 | 10.2 | 22.9 |

Notes: Note that some sites could not be sampled in certain seasons due to access limitations or were removed from the model as their values fell outside the mixing polygon (typically due to high electrical conductivity readings).

the source of groundwater, we used the mean annual precipitation values from OIPC to model the predicted recharge elevation of the groundwater sites, following the methods outlined in Jeelani, Bhat, and Shivanna (2010) and Kanduč et al. (2012). Predicted recharge elevations ranged from 970 masl to 2940 masl and averaged 2000 masl (Table S.3.1). The predicted recharge elevation of the groundwater sites was consistent between seasons, with the exception of site 93, which is a shallow well with strong connection to the river and had a lower elevation predicted recharge zone in the spring and summer than fall. Based on the predicted recharge elevations, the groundwater sites are likely being recharged from the high elevation snowpack in the bordering mountains ranges. Interannual similarity of isotope precipitation patterns precludes us from determining when groundwater recharge from snowmelt may have occurred.

## Proportion of wetland water attributed to input sources

To determine the proportion of wetland water contributed by groundwater, river water, and rainfall, a three-component mixing model was deployed using $\delta^{18}O$, $\delta^2H$ and electrical conductivity as tracers. During Spring, three sites (site 30, 35 and 84) plotted outside of the mixing polygon defined by the input sources and were therefore unsuitable for analysis and removed (Philips et al. 2014). Wetlands mainly contained river water and groundwater during the spring (Figure 4), with a mean proportion of 47% river water (+/− 0.16 sd), 32% groundwater (+/− 0.12 sd) and 17% precipitation (+/− 0.09 sd). Wetlands varied widely in terms of the relative contributions of river and groundwater sources, but contained little precipitation (Figure 4). Given our hypothesis that spring groundwater is primarily derived from snowmelt, this
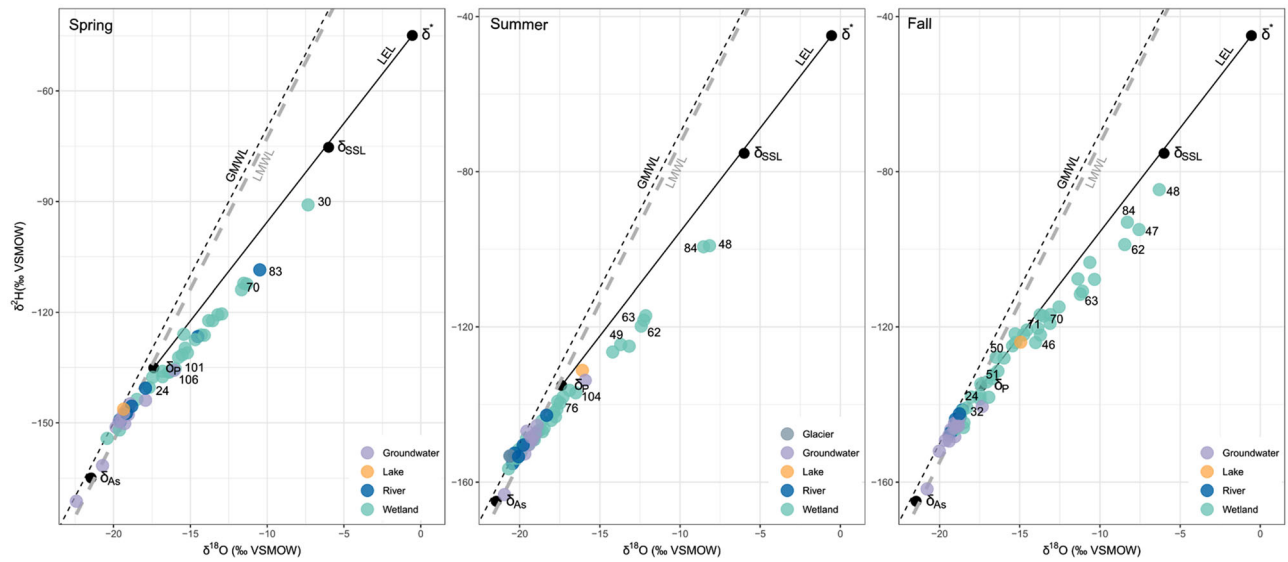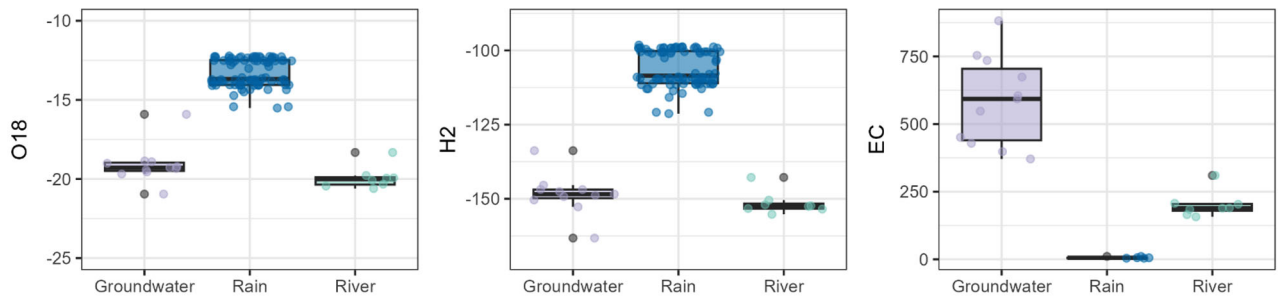
**Figure 2.** $\delta^{18}$O-$\delta^2$H Graphs showing the water isotope compositions of the river, groundwater, wetlands and Columbia Lake in the Columbia Valley, British Columbia, sampled in (a) spring, (b) summer and (c) fall of 2019.
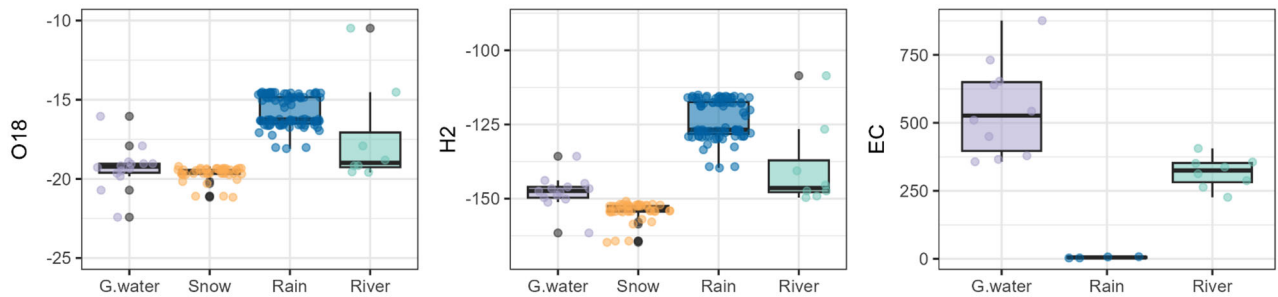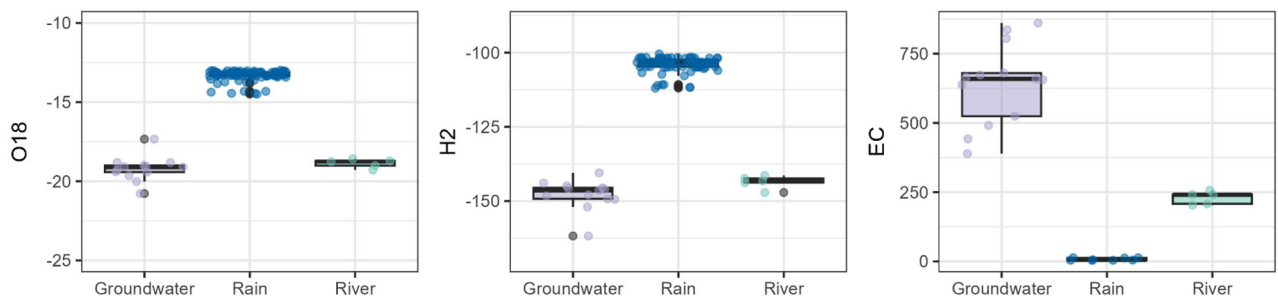


**Figure 3.** Boxplots of $\delta^{18}$O, $\delta^2$H and electrical conductivity (EC) values of the groundwater, snow, rain and river water in the Columbia River Valley during the spring (top panels), summer (Middle panels) and fall of 2019 (bottom panels). River and groundwater samples were collected at representative locations, while snow and rain are modelled values obtained from the OIPC v3.2 data base.
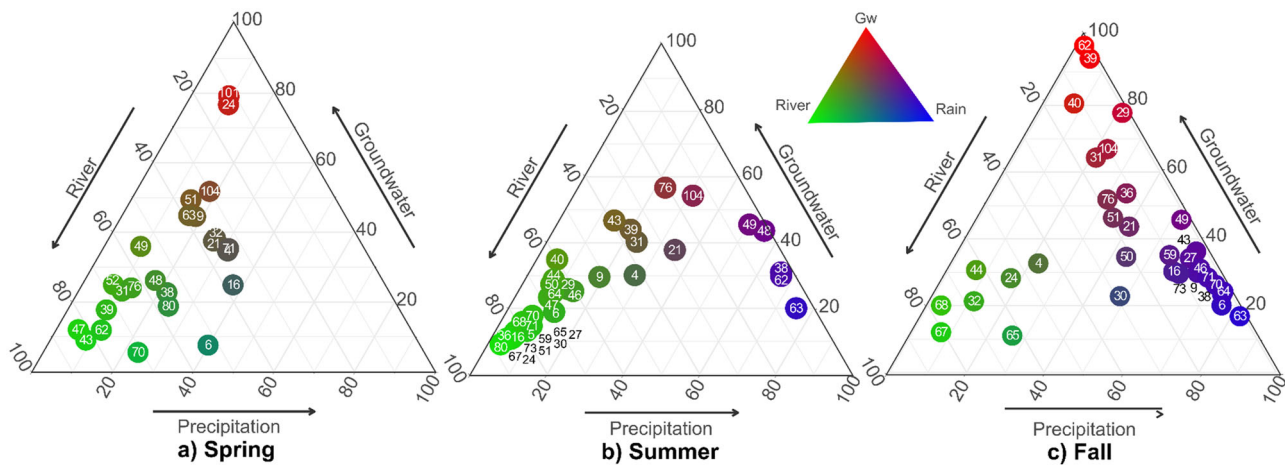
**Figure 4.** Tertiary plots showing the proportion of water attributed to groundwater by Bayesian mixing model in wetlands in the upper Columbia Valley sampled in the spring (a), summer (b) and fall (c) of 2019.

suggests winter precipitation is important to retaining spring water levels in many of the wetlands.

During summer, three sites (site 35, 84 and 101) plotted outside of the mixing polygon and were removed. In each case the site electrical conductivity was substantially higher than the electrical conductivity of the input sources. The proportion of wetland water contributed by river water increased in the summer to an average of 56% (+/− 0.13 sd), while the average groundwater proportion decreased to 25% (+/− 0.13 sd) and the average proportion of precipitation remained the same at 18% (+/− 0.5 sd). At sites 62, 63, 38 and 48, the importance of precipitation increased substantially, whereas most wetlands were dominated by river water inputs (Figure 4).

During the fall, six sites plotted outside the mixing polygon and were removed from further analysis (site 35, 47, 48, 62, 84 and 101). The proportion of wetland water contributed by river water decreased at all sites, averaging only 21% (+/− 0.07 sd), while the average groundwater proportion increased to 38% (+/− 0.08 sd) and the average precipitation proportion increased to 41% (+/− 0.5 sd). Sites varied widely in the relative importance of groundwater (which dominated sites like 39 and 40) vs. precipitation (which dominated sites like 62 and 6; Figure 4).

### Spatial pattern in evaporation to inflow ratio

No significant spatial autocorrelation was detected in E/I's during any of the 2019 sampling periods. Most wetlands had E/$I < 0.5$ in the spring, indicating they are inflow dominated (Tondu et al. 2013, MacDonald et al. 2016). Only site 30 (E/I = >1) and site 70 (E/$I = 0.56$) were evaporation dominated in the spring. In the summer, only sites 48 and 84 were

evaporation dominated (E/I =>1), while all other sites were inflow dominated. In the fall, wetlands 48 and 84 remained evaporation-dominated, and sites 47, 62, and 63 also became evaporation-dominated.

### Discussion

As climate change alters hydrologic patterns, many sensitive wetland environments are threatened with decreased water input. In the Columbia River wetlands, where the area of open water has already been reduced by decreased snowpack (Hopkinson et al. 2020), altered hydrology is expected to have cascading effects on vegetation and biota (Rooney, Carli, and Bayley 2013, Carli and Bayley 2015). Quantifying the relative contributions of the main input water sources to wetlands throughout the ice-free season provides an important new understanding of hydrologic connectivity and improves our ability to predict the future effect on wetlands of shifts in the availability of each water source. In this study, we found there was strong seasonality of input water sources across the ice-free season. The wetlands were primarily sustained by a mix of groundwater and/or river water in the spring, by river water during the summer peak flow and by rainfall and/or groundwater in the fall (Figure 4).

We hypothesized that snowmelt would be important in the spring, and our results largely support our hypothesis. We found that groundwater was primarily derived from alpine snowmelt (Figure 3) originating in the surrounding mountain ranges and was an important source of input water to several wetlands, particularly in the spring and fall (Figure 4). This aligns with the research on mountain block recharge, which describes the importance of high-elevation

watershed in recharging groundwater that feeds stream and river headwaters (Hayashi 2020; Wilson and Guan 2004; Markovich et al. 2019). Most of the wetlands had both groundwater and river water as major water input sources. Exceptions include sites like 101, which is known to be groundwater fed in the absence of large floods and was found to have groundwater as the strongly predominant water input source. Site 24 was also predominately fed by groundwater, which aligns with observations that the wetland is connected to an upland spring.

Our hypothesis that river water plays a dominant role in wetland water budgets in the summer was well supported by our results. A majority of the wetlands had >50% river water, which aligns with the summer flood peak. The main river pulse was the dominant input water source in the summer, even though the river water did not overtop the levees in 2019. For the majority of sites, levee gaps and channels are presumably sufficient to recharge wetlands. Some exceptions include sites 62, 63, 38, 48 and 49 which have reduced connections to the main river, site 24 which is an upland site, and site 104 which is spring-fed and therefore groundwater-dominated. These results agree with the wetland categorizations reported in MacDonald and Chernos (2020).

We predicted an increased importance of groundwater in the fall, however we found both groundwater and rainfall contributed to the water balances of the majority of wetlands at this time. Exceptions include sites 32, 65, 67 and 68 which are all located close to the Columbia River and are easily flooded by river water, so the large contribution of river water to these wetlands during all seasons, including the fall, is not surprising. The predominance of rainfall in most sites aligns with meteorological records indicating large rainfall events in the week prior to as well as during the fall sampling period. The contribution of groundwater to sites in the fall indicates additional support for the conclusion that groundwater derived from mountain snowmelt is an important component of the wetland water balances. Given this, groundwater residence times and flow paths are important questions for further study.

We hypothesized that there would be a spatial relationship between the influence of evaporation on the wetland water balance and the wetland's distance from the main river stem; however, we did not detect any significant spatial pattern in isotope composition. This aligns with the findings of Hopkinson et al. 2020, which showed that decreases in permanent open water during 2003-2019, compared to 1984-

2002, were located throughout the Columbia River Valley and were not spatially clustered in any notable way. The majority of the wetlands had a low E/I value, indicative of greater water input than evaporative losses.

The inclusion of additional water chemistry tracers would aid in distinguishing the input sources, and potentially improve the reliability of the model. For example, analysis of major ions, such as Na and Cl, has been shown to be useful in distinguishing groundwater from surface water (Baskaran et al. 2009). Additional stable isotope-based research to better resolve the relationship between precipitation and groundwater would be useful in this landscape, as would further investigation into the residence time of the groundwater. However, the model presented here largely aligns with our knowledge of the individual wetlands sampled and provides a robust 'first cut' at determining the relative contributions of source waters to wetland water budgets in the Columbia River wetlands. Our water isotope and electrical conductivity-based approach allowed us to distinguish between three key input water sources, and provides important new understanding about the contributions of groundwater to wetland recharge and the seasonal variability of these inputs.

Given predicted decreases in precipitation in the Columbia River Valley and reductions in river flow (Rood et al. 2016), the relative contributions of input water sources may be expected to shift over time, with increasing reliance on groundwater to sustain wetland ecosystems. Groundwater in similar landscapes has been found the have long hydraulic memory (Cuthbert et al. 2019) and relatively long residence times (Hayashi 2020). The delayed response between declining alpine snowpack and groundwater availability, however, may increase the likelihood of groundwater overallocation, resulting in long term loss of groundwater input essential to sustaining these habitats. This has ecological implications, as these wetlands are known to be important stopover habitat for many migratory birds and the region is currently under consideration by BirdLife International for designation as an Important Bird Area (pers. com. R. Darvill 2022). There are substantial differences in the amount of groundwater between different wetlands that may relate to their position in the floodplain, the number and size of the gaps in the levees, the activity of beavers and other geomorphological processes. Under predicted climate change induced increases in discharge during the winter and spring season in the Upper Columbia River Valley, and decreased

discharge during the summer (Werner et al. 2013), wetlands may become increasingly reliant on groundwater and precipitation-derived water input sources as peak river flow declines. Improving our understanding of the role of groundwater on these ecosystems is therefore imperative to making informed management and conservation decisions.

## Acknowledgements

## Disclosure statement

No potential conflict of interest was reported by the authors.

## ORCID

Casey R. Remmer http://orcid.org/0000-0003-2626-3012
Rebecca Rooney http://orcid.org/0000-0002-3956-7210
Suzanne Bayley http://orcid.org/0000-0002-0663-8801

## Data availability statement

The authors confirm that the data supporting the findings of this study are available within the article.

## References

Baskaran, S., T. Ransley, R. S. Brodie, and P. Baker. 2009. "Investigating Groundwater–River Interactions Using Environmental Tracers." *Australian Journal of Earth Sciences* 56 (1): 13–19. https://doi.org/10.1080/08120090802541887

Blasch, K. W., and J. R. Bryson. 2007. "Distinguishing Sources of Ground Water Recharge by Using δ2H and δ18O." *Ground Water* 45 (3): 294–308. https://doi.org/10.1111/j.1745-6584.2006.00289.x

Bowen, G. J. 2016. "The Online Isotopes in Precipitation Calculator, version 2.2." http://www.waterisotopes.org.

Bowen, G. J., and J. Revenaugh. 2003. "Interpolating the Isotopic Composition of Modern Meteoric Precipitation." *Water Resources Research* 39 (10): 1299. https://doi.org/10.1029/2003WR002086

Bowen, G. J., L. I. Wassenaar, and K. A. Hobson. 2005. "Global application of stable hydrogen and oxygen isotopes to wildlife forensics." *Oecologia* 143: 337–348. https://doi.org/10.1007/s00442-004-1813-y

Brahney, J., F. Weber, V. Foord, J. Janmaat, and P. J. Curtis. 2017. "Evidence for a Climate-Driven Hydrologic Regime Shift in the Canadian Columbia Basin." *Canadian Water Resources Journal/Revue Canadienne Des Ressources Hydriques* 42 (2): 179–192. https://doi.org/10.1080/07011784.2016.1268933

Brock, B. E., B. B. Wolfe, and T. W. D. Edwards. 2007. "Characterizing the Hydrology of Shallow Floodplain Lakes in the Slave River Delta, NWT, Canada, Using Water Isotope Tracers." *Arctic, Antarctic, and Alpine Research* 39 (3): 388–401. https://doi.org/10.1657/1523-0430(06-026)[BROCK]2.0.CO;22.0.CO;2]

Brock, B. E., B. B. Wolfe, and T. W. D. Edwards. 2008. "Spatial and Temporal Perspectives on Spring Break-up Flooding in the Slave River Delta, NWT." *Hydrological Processes* 22 (20): 4058–4072. https://doi.org/10.1002/hyp.7008

Carli, C. M., and S. E. Bayley. 2015. "River Connectivity and Road Crossing Effects on Floodplain Vegetation of the Upper Columbia River, Canada." *Écoscience* 22 (2-4): 97–107. https://doi.org/10.1080/11956860.2015.1121705

Columbia Wetland Stewardship Partners. 2009. "Upper Columbia River Watershed Hydrometric Analysis – Phase 1." https://engage.gov.bc.ca/app/uploads/sites/71/2013/10/Columbia-Wetland-Stewardship-Partners.pdf

Cooper, D. J., R. Chimner, and D. Merritt. 2012. "Western Mountain Wetlands." *Chapter 22, in: Wetland Habitats of North America: Ecology and Conservation Concerns*. edited by: Darold P. Batzer and Andrew H. Baldwin, 313–328. Oakland, CA, USA: University of California Press.

Coplen, T. B. 1996. "New Guidelines for Reporting Stable Hydrogen, Carbon, and Oxygen Isotope-Ratio Data." *Geochimica et Cosmochimica Acta* 60 (17): 3359–3360. https://doi.org/10.1016/0016-7037(96)00263-3

Craig, H., and L. I. Gordon. 1965. "Deuterium and Oxygen 18 Variations in the Ocean and the Marine Atmosphere." In *Stable Isotopes in Oceanographic Studies and Paleotemperatures. Laboratorio di Geologia Nucleare*, edited by E. Tongiorgi, p. 9–130. Italy: Pisa.

Cuthbert, M. O., T. Gleeson, N. Moosdorf, K. M. Befus, A. Schneider, J. Hartmann, and B. Lehner. 2019. "Global Patterns and Dynamics of Climate–Groundwater Interactions." *Nature Climate Change* 9 (2): 137–141. https://doi.org/10.1038/s41558-018-0386-4

Edwards, T. W. D., B. B. Wolfe, J. J. Gibson, and D. Hammarlund. 2004. "Use of Water Isotope Tracers in High Latitude Hydrology and Paleolimnology." In *Long-Term Environmental Change in Arctic and Antarctic Lakes*, edited by R. Pienitz, M. S. V. Douglas, and J. P. Smol, 187–207. Dordrecht, Netherlands: Springer.

Filgueira-Rivera, M., N. Smith, and R. Slingerland. 2007. "Controls on Natural Levee Development in the Columbia River, British Columbia, Canada." *Sedimentology* 54 (4): 905–919. https://doi.org/10.1111/j.1365-3091.2007.00865.x

Gibson, J. J., and T. W. D. Edwards. 2002. "Regional Water Balance Trends and Evaporation-Transpiration Partitioning from a Stable Isotope Survey of Lakes in Northern Canada." *Global Biogeochemical Cycles* 16 (2): 10–1–10-14. https://doi.org/10.1029/2001GB001839

Gonfiantini, R. 1986. "Environmental Isotopes in Lake Studies." In *Handbook of Environmental Isotope Geochemistry*, edited by P. Fritz & J. C. Fontes, Vol. 2, 113–168. . New York: Elsevier.

Hare, F. K., and M. K. Thomas. 1974. *Climate Canada*. Toronto: Wiley Publishers.

Hayashi, M. 2020. "Alpine Hydrogeology: The Critical Role of Groundwater in Sourcing the Headwaters of the

World." *Ground Water* 58 (4): 498–510. https://doi.org/10.1111/gwat.12965

Hopkinson, C., B. Fuoco, T. Grant, S. E. Bayley, B. Brisco, and R. MacDonald. 2020. "Wetland Hydroperiod Change along the Upper Columbia River Floodplain, Canada, 1984 to 2019." *Remote Sensing* 12 (24): 4084. https://doi.org/10.3390/rs12244084

Horita, J., and D. Wesolowski. 1994. "Liquid-Vapour Fractionation of Oxygen and Hydrogen Isotopes of Water from the Freezing to the Critical Temperature." *Geochimica et Cosmochimica Acta* 58 (16): 3425–3437. https://doi.org/10.1016/0016-7037(94)90096-5

Huntington, J. L., and R. G. Niswonger. 2012. "Role of Surface-Water and Groundwater Interactions on Projected Summertime Streamflow in Snow Dominated Regions: An Integrated Modeling Approach." *Water Resources Research* 48 (11): W11524. https://doi.org/10.1029/2012WR012319

IAEA/WMO. 2015. "Global Network of Isotopes in Precipitation. The GNIP Database." https://nucleus.iaea.org/wiser.

Jeelani, G., N. A. Bhat, and K. Shivanna. 2010. "Use of d18O Tracer to Identify Stream and Spring Origins of a Mountainous Catchment: A Case Study from Liddar Watershed, Western Himalaya, India." *Journal of Hydrology* 393 (3–4): 257–264. https://doi.org/10.1016/j.jhydrol.2010.08.021

Kanduč, Tjaša, Nataša Mori, David Kocman, Vekoslava Stibilj, and Fausto Grassa. 2012. "Hydrogeochemistry of Alpine Springs from North Slovenia: Insights from Stable Isotopes." *Chemical Geology* 300-301: 40–54. https://doi.org/10.1016/j.chemgeo.2012.01.012

Kay, M. L., H. K. Swanson, J. Burbank, T. J. Owca, L. A. MacDonald, C. A. M. Savage, C. R. Remmer, et al. 2021. "A Bayesian Mixing Model Framework for Quantifying Temporal Variation in Source of Sediment to Lakes across Broad Hydrological Gradients of Floodplains." *Limnology and Oceanography: Methods* 19 (8): 540–551. https://doi.org/10.1002/lom3.10443

MacDonald, R., and M. Chernos. 2020. *Hydrological Assessment of the Upper Columbia River Watershed*, 64. Cranbrook, BC, Canada: MacHydro Consultants Ltd.

MacDonald, L. A., B. B. Wolfe, K. W. Turner, L. Anderson, C. D. Arp, S. J. Birks, F. Bouchard, et al. 2016. "A Synthesis of Thermokarst Lake Water Balance in High-Latitude Regions of North America from Isotope Tracers." *Arctic Science* 3 (2): 118–149. https://doi.org/10.1139/as-2016-0019

Makaske, B., D. G. Smith, H. J. A. Berendsen, A. G. de Boe, M. F. van Nielen-Kiezebrink, and T. Locking. 2009. "Hydraulic and Sedimentary Processes Causing Anatomosing Morphology of the Upper Columbia River, British Columbia, Canada." *Geomorphology* 111 (3–4): 194–205. https://doi.org/10.1016/j.geomorph.2009.04.019

Markovich, K., H. Manning, A. H. Condon, and J. C. McIntosh. 2019. "Mountain-Block Recharge: A Review of Current Understanding." *Water Resources Research* 55 (11): 8278–8304. https://doi.org/10.1029/2019WR025676

Messerli, B., D. Viviroli, and R. Weingartner. 2004. "Mountains of the World: Vulnerable Water Towers for the 21st Century." *Ambio* Spec No 13: 29–34. http://www.jstor.org/stable/25094585. https://doi.org/10.1007/0044-7447-33.sp13.29

Mote, P. W., S. Li, D. P. Lettenmaier, M. Xiao, and R. Engel. 2018. "Dramatic Declines in Snowpack in the Western US." *Climate and Atmospheric Science* 1 (1): 1–6. https://doi.org/10.1038/s41612-018-0012-1

Mote, P. W., A. F. Hamlet, M. P. Clark, and D. P. Lettenmaier. 2005. "Declining Mountain Snowpack in Western North America." *Bulletin of the American Meteorological Society* 86 (1): 39–50. https://doi.org/10.1175/BAMS-86-1-39

NEON (National Ecological Observatory Network. 2021. "Wet deposition chemical analysis, RELEASE-2021 (DP1.00013.001)." https://doi.org/10.48443/w1kw-re18Accessed September 29, 2021. https://data.neonscience.org.

Parnell, A. C., R. Inger, S. Bearhop, and A. L. Jackson. 2010. "Source Partitioning Using Stable Isotopes: Coping with Too Much Variation." *PloS One* 5 (3): e9672. https://doi.org/10.1371/journal.pone.0009672

Parnell, A. C., D. L. Phillips, S. Bearhop, B. X. Semmens, E. J. Ward, J. W. Moore, A. L. Jackson, J. Grey, D. J. Kelly, and R. Inger. 2013. "Bayesian Stable Isotope Mixing Models." *Environmetrics* 24 (6): n/a–n/a. https://doi.org/10.1002/env.2221

Phillips, D. L., R. Inger, S. Bearhop, A. L. Jackson, J. W. Moore, A. C. Parnell, B. X. Semmens, and E. J. Ward. 2014. "Best practices for use of stable isotope mixing models in food-web studies." *Canadian Journal of Zoology* 92 (10): 823–835. https://doi.org/10.1139/cjz-2014-0127

Remmer, C. R., T. Owca, L. N. Neary, J. A. Wiklund, M. Kay, B. B. Wolfe, and R. I. Hall. 2020a. "Delineating Extent and Magnitude of River Flooding to Lakes across a Northern Delta Using Water Isotope Tracers." *Hydrological Processes* 34 (2): 303–320. https://doi.org/10.1002/hyp.13585

Remmer, C. R., L. N. Neary, M. Kay, B. B. Wolfe, and R. I. Hall. 2020b. "Multi-Year Isoscapes of Lake Water Balances across a Dynamic Northern Freshwater Delta." *Environmental Research Letters* 15 (10): 104066. https://doi.org/10.1088/1748-9326/abb267

Rooney, R. C., C. M. Carli, and S. E. Bayley. 2013. "River Connectivity Affects Submerged and Floating Aquatic Vegetation in Floodplain Wetlands." *Wetlands* 33 (6): 1165–1177. https://doi.org/10.1007/s13157-013-0471-4

Rood, S. B., S. G. Foster, E. J. Hillman, A. Luek, and K. P. Zanewich. 2016. "Flood Moderation: Declining Peak Flows along Some Rocky Mountain Rivers and the Underlying Mechanism." *Journal of Hydrology* 536: 174–182. https://doi.org/10.1016/j.jhydrolo.2016.02.043

Schnorbus, M., A. Werner, and K. Bennett. 2014. "Impacts of Climate Change in Three Hydrologic Regimes in British Columbia, Canada." *Hydrological Processes* 28 (3): 1170–1189. https://doi.org/10.1002/hyp.9661

Somers, L. D., and J. M. McKenzie. 2020. "A Review of Groundwater in High Mountain Environments." *WIREs Water.* 7 (6): e1475. https://doi.org/10.1002/wat2.1475

Thornthwaite, C. W. 1948. "An Approach toward a Rational Classification of Climate." *Geographical Review* 38 (1): 55–94. https://doi.org/10.2307/210739

Tondu, J. M. E., K. W. Turner, B. B. Wolfe, R. I. Hall, T. W. D. Edwards, and I. McDonald. 2013. "Using water isotope tracers to develop the hydrological component of a long-term aquatic ecosystem monitoring program for a northern lake-rich landscape." *Arctic, antarctic, and alpine research* 45 (4): 594–614. https://doi.org/10.1657/1938-4246-45.4.594

Turner, K. W., B. B. Wolfe, T. W. D. Edwards, T. C. Lantz, R. I. Hall, and G. Larocque. 2014. "Controls on Water Balance of Shallow Thermokarst Lakes and Their Relations with Catchment Characteristics: A Multi-Year, Landscape-Scale Assessment Based on Water Isotope Tracers and Remote Sensing in Old Crow Flats, Yukon (Canada)." *Global Change Biology* 20 (5): 1585–1603. https://doi.org/10.1111/gcb.12465

Utzig, G. 2021. "The Columbia Wetlands and Climate Disruption." Nature Investigations Ltd. Nelson, BC. https://kootenayconservation.ca/wp-content/uploads/2021/06/Kootenay-Connect-Y2-Final-Report-09June2021.pdf

Upper Columbia Basin Groundwater Monitoring Program (UCBGMP). 2021. "2020 Data Collection Summary." https://livinglakescanada.ca/wp-content/uploads/2021/08/2020-llc-groundwater-monitoring-program-data-summary_final-report_v2.pdf.

Yi, Y., Brock, B. E. Falcone, M. D. Wolfe, B. B. T. W. D, and Edwards, T. W. D. 2008. "A Coupled Isotope Tracer Method to Characterize Input Water to Lakes." *Journal of Hydrology* 350 (1-2): 1–13. https://doi.org/10.1016/j.jhydrol.2007.11.008

Wassenaar, L. I., P. Athanasopoulos, and M. J. Hendry. 2011. "Isotope Hydrology of Precipitation, Surface and Ground Waters in the Okanagan Valley, British Columbia, Canada." *Journal of Hydrology* 411 (1-2): 37–48. https://doi.org/10.1016/j.jhydrol.2011.09.032

Werner, A. T., M. A. Schnorbus, R. R. Shrestha, and H. D. Eckstrand. 2013. "Spatial and Temporal Change in the Hydro-Climatology of the Canadian Portion of the Columbia River Basin under Multiple Emissions Scenarios." *Atmosphere-Ocean* 51 (4): 357–379. https://doi.org/10.1080/07055900.2013.821400

Wilson, J. L., and H. Guan. 2004. "Mountain-Block Hydrology and Mountain-Front Recharge." In *Groundwater Recharge in a Desert Environment, the Southwestern United States*, edited by F. Phillips, J. Hogan, & B. Scanlon Washington, DC: AGU. https://doi.org/10.1029/009WSA08

Wolfe, Brent B., Roland I. Hall, Thomas W. D. Edwards, Sheila R. Vardy, Matthew D. Falcone, Charlotte Sjunneskog, Florence Sylvestre, Suzanne McGowan, Peter R. Leavitt, and Peter van Driel. 2008. "Hydroecological Responses of the Athabasca Delta, Canada, to Changes in River Flow and Climate during the 20th Century." *Ecohydrology* 1 (2): 131–148. https://doi.org/10.1002/eco.13

Wynants, M., G. Millward, A. Patrick, A. Taylor, L. Munishi, K. Mtei, L. Brendonck, et al. 2020. "Determining Tributary Sources of Increased Sedimentation in East-African Rift Lakes." *The Science of the Total Environment* 717: 137266. https://doi.org/10.1016/j.scitotenv.2020.137266

Zuecco, G., L. Carturan, F. De Blasi, R. Seppi, T. Zanoner, D. Penna, M. Borga, A. Carton, and G. Dalla Fontana. 2018. "Understanding Hydrological Processes in Glacierized Catchments: Evidence and Implications of Highly Variable Isotopic and Electrical Conductivity Data." *Hydrological Processes* 33: 816–832. https://doi.org/10.1002/hyp.13366